Int J Adv Manuf Technol (2015) 76:1769–1781
DOI 10.1007/s00170-014-6312-7

ORIGINAL ARTICLE

Optimization of process parameters in twin-roll strip casting of an AZ61 alloy by experiments and simulations

J. T. Li · G. M. Xu · H. L. Yu · G. Y. Deng · L. H. Su · C. Lu · L. Z. He · A. Godbole · H. J. Li

Received: 30 November 2012 / Accepted: 21 August 2014 / Published online: 26 September 2014

Abstract Twin-roll strip casting is an effective technology to produce magnesium alloy strips economically. The aim of this work is to propose suitable (optimized) process parameters for manufacturing AZ61 strips using the twin-roll strip casting technology. Experiments on twin-roll strip casting of an AZ61 magnesium alloy were carried out. Temperature fields, fluid flow fields, and stress fields accompanying the process were simulated using thermal-fluid and thermal-mechanical finite element methods. The effects of casting speed and pouring temperature on temperature fields, fluid flow fields, and stress fields during the process were analyzed. It was found that the optimum pouring temperature should be in the range 690~715 °C and the optimum casting speed in the range 2.3 and 2.5 m/min.

Keyword AZ61 alloy · Twin-roll strip casting · Pouring temperature · Casting velocity · Numerical simulation

J. T. Li · G. M. Xu (✉) · L. Z. He
Key Laboratory of Electromagnetic Processing of Materials (Ministry of Education), Northeastern University, Shenyang 110819, People's Republic of China
e-mail: xu_gm@epm.neu.edu.cn

J. T. Li · H. L. Yu (✉) · G. Y. Deng · L. H. Su · C. Lu · A. Godbole · H. J. Li
School of Mechanical, Materials and Mechatronic Engineering, University of Wollongong, Wollongong, NSW 2500, Australia
e-mail: hailiang@uow.edu.au

H. L. Yu
e-mail: yuhailiang1980@tom.com

G. Y. Deng
State Key Lab of Rolling and Automation, Northeastern University, Shenyang 110819, People's Republic of China

L. H. Su
School of Materials and Metallurgy, Northeastern University, Shenyang 110819, People's Republic of China

1 Introduction

Reduction of total product weight and carbon dioxide emission are objectives that an increasing number of manufacturers strive for [1, 2]. Magnesium alloys can have particularly desirable strength-to-weight ratios. The density of magnesium alloys is about 2/3 that of aluminum alloys and 1/4 that of steel. Magnesium alloys have high specific strength and stiffness, good damping characteristics, acceptable weldability, and excellent machinability. They also have excellent shielding capability against electromagnetic interference, good environmental stability, and effective heat dissipation. Magnesium alloys are therefore expected to be used in an increasing number of applications in the future.

However, high manufacturing cost is a major obstacle that prevents widespread use of magnesium alloys. The twin-roll strip casting technology is a method to economically manufacture magnesium alloy strips of high quality [3–6]. The biggest advantage of the technology is that it produces magnesium alloy strips having the desired thickness directly from the molten metal, thereby reducing capital investment and operational costs compared with conventional processes. Due to this advantage, the twin-roll strip casting technique has assumed increasing importance over the last 40 years.

The suitability of the twin-roll strip casting process for magnesium alloys has been widely investigated, particularly in case of AZ31 alloys. Appropriate strip casting and manufacturing conditions have been proposed, and the formability of strips that were hot rolled after casting has been investigated [7–9]. Addition of calcium in the molten alloy during twin-roll strip casting was found to significantly reduce the average grain size of thin AZ31 strips [10]. Masoumi et al. [11] investigated the microstructures and textures of twin-roll strip cast AZ31 strips. Asymmetric twin-roll strip casting of AZ31 alloys has also been investigated [12, 13]. Melt conditioning by intensive shear prior to twin-roll strip casting of

AZ31 magnesium alloy was used to promote heterogeneous nucleation and to provide a refined and uniform microstructure without severe macro-segregation [14]. However, twin-roll strip casting of AZ61 alloys has not been widely investigated to date. Mino et al. [15] cast AZ61 strips using a twin-roll caster and investigated the effects of casting conditions and rolling parameters on the surface features. Watari et al. [9] investigated the appropriate strip casting manufacturing conditions for AZ61 magnesium alloy. Liang and Cowley [16] have described the challenges faced in producing of magnesium alloy strips by twin-roll strip casting.

An investigation of the solidification behavior during twin-roll strip casting is essential to improve the quality of cast strips. Furthermore, the influence of casting parameters such as pouring temperature and casting velocity on the solidification must be considered. Several numerical models that can lead to a better understanding of the process have been suggested. Hwang et al. [17] suggested that a constant heat transfer coefficient could be used in their computational fluid dynamics (CFD) model to describe the heat transfer between the metal and the rollers. Santos et al. [18] described a numerical model for the two-dimensional solidification problem in twin-roll strip casting by using a finite difference technique. Lin [19] proposed a mathematical model and numerical algorithm based on a continuum model for conservation of mass, momentum, and energy to deal with the phenomena of fluid flow, heat transfer, and partial solidification. Ju et al. [20] analyzed the process conditions for a twin-roll caster by thermal flow simulation. Miao et al. [21] developed a coupled three-dimensional flow and heat transfer model to simulate the twin-roll strip casting process using a finite element method. Bae et al. [22] examined the velocity and temperature fields during the vertical twin-roll strip casting of Mg by a 2D finite difference method (FDM) and a finite element method (FEM). Zeng et al. [23] developed a CFD model for the twin-roll strip casting process for magnesium alloy. Temperature and fluid flow fields in the cast-rolling zone have been studied using a coupled finite element method [24].

Specialized roll casting technology has received considerable attention, but normal roll casting technology has been relatively neglected. This paper describes research focused on developing a twin-roll casting technology for magnesium alloys. The technique uses the widely used twin-roll strip caster and adapts the existing strip caster technology to make it more suitable for the production of magnesium alloy strips.

During twin-roll strip casting, the process parameters such as pouring temperature, casting velocity, water velocity, water temperature, rolling pressure, nozzle size, and roller gap will affect the quality of the product. Among these processing parameters, Li et al. [25–27] have obtained a suitable value of the nozzle size and the roller gap which allows the manufacture of 400-mm wide strips. In this paper, twin-roll strip casting experiments on an AZ61 magnesium alloy are described, along with an FEM model of the twin-roll strip casting process. An investigation of the strip quality resulting from a variety of process parameters (pouring temperature and casting speed) was carried out based on previous studies [25–27]. The methodology of this research consists of obtaining both visual impressions and objective data through twin-roll strip casting experiments and then simulating the process to validate experimental results and analyzing the influence of process parameters on the solidification process. The simulation results provide a better understanding of the melt flow characteristics and heat transfer effects during the rapid solidification process. Finally, a discussion of the

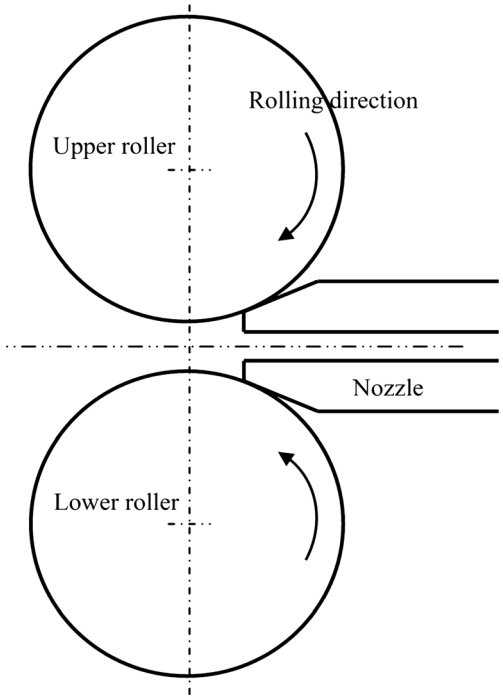

Fig. 1 Schematic diagram of nozzle and rollers

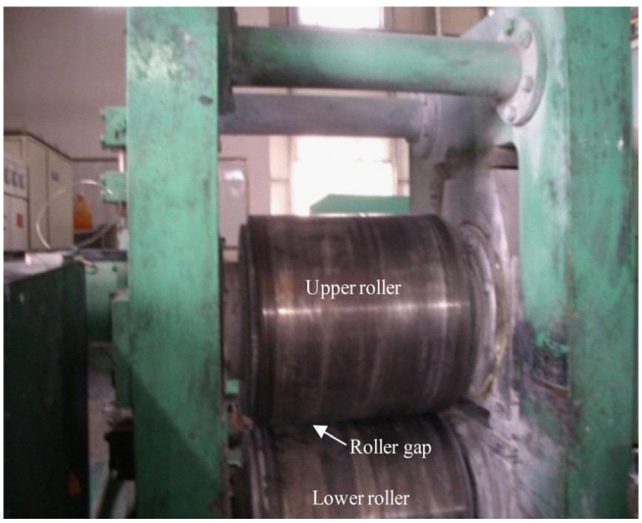

Fig. 2 Reversible twin-roll strip caster

Table 1 Dimensions of twin-roll strip caster

Diameter of upper roller	Diameter of lower roller	Minimum casting speed	Maximum casting speed
500 mm	500 mm	0.5 m/min	7 m/min

influence of the casting speed and the pouring temperature on the solidification process is presented.

2 Experimental investigation

The experimental arrangement includes a melting furnace, a nozzle, and a reversible twin-roll strip caster. The hearth of the melting furnace is made of heat-resistant steel, with an orifice at the bottom. Appropriate positioning of the nozzle with respect to the orifice ensures that no impurities enter the nozzle during the operation. Shielding gas enters the furnace through a hole in the top cover. A schematic diagram of nozzle and rollers is shown in Fig. 1. The twin-roll strip caster has two counter-rotating rollers, which are water-cooled from the inside. The roller shell is made of heat-resistant alloy steel. The roller gap is adjusted by hydraulic pressure. The reversible twin-roll strip caster is shown in Fig. 2, and its dimensions are listed in Table 1.

Figure 3 presents a flow chart of the melting process of AZ61 magnesium alloy. An AZ61 magnesium alloy (composed of 6 % Al, 1 % Zn, 0.2 % Mn, 0.2 % Ca, and 92.6 % Mg) was used in the twin-roll strip casting experiments. First, commercially pure magnesium and aluminum were put in the furnace and melted completely. During the heating process, the melt was immersed in a protective atmosphere of SF_6 and CO_2 gas mixture. Then, commercially pure zinc and Al-9 % Mn master alloy was added to the melt. After stirring uniformly, 0.2 % Ca was added into magnesium alloy liquid to achieve effective flame retardation. The furnace temperature was controlled in the range 680~750 °C. This was followed by standing and filtration. When the temperature reached the preset value, the twin-roll strip casting experiment commenced. In the experiment, the rolling pre-pressure was 7 MPa, the roller water pressure was 0.2 MPa, and water flow was 5 m^3/h. The casting speed and pouring temperature were the two main variables. In this research, two groups of experiments were conducted: (1) variable pouring temperature with fixed casting velocity and (2) variable casting speed with fixed pouring temperature. Higher pouring temperature demands more radiating time (constant water flow), which in turn requires lower casting velocity to achieve the desired result. Similarly, higher casting velocity causes a reduction in the radiating time, which necessitates lower pouring temperature. It is thus seen that increasing or decreasing these two variables simultaneously is likely to worsen the quality of the resulting AZ61 magnesium alloy strips.

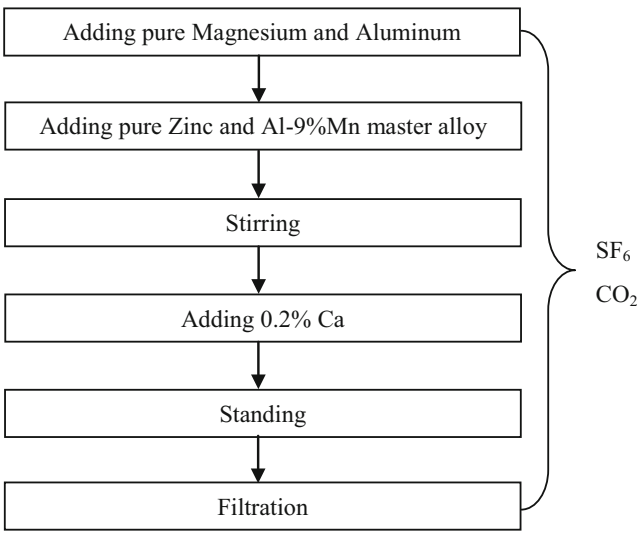

Fig. 3 Flow chart of the melting process of AZ61 magnesium alloy

After fabrication, the surface texture of the strips was examined by visual inspection since prominent macro-defects are easily noticeable.

3 Process simulation

3.1 Process and physical performance parameters

The computational domain in the simulated physical model consisted of the magnesium melt in the nozzle and the roll-casting zone. The following simplifying assumptions were made:

(1) The high-temperature magnesium alloy melt was assumed to behave like an incompressible Newtonian fluid;
(2) Influence of the solidification shell on the flow was neglected in the roll-casting zone;

Table 2 Process parameters of twin-roll strip caster

Parameter	Numerical value
Roll diameter (m)	0.5
The width of roller (m)	0.5
Strip thickness (m)	0.005
Biting angle (°)	15
Pouring temperature (°C)	680, 700, 720
Casting velocity (m min^{-1})	1.8, 2.4, 3.0
Convective heat transfer coefficient (W m^{-2} °C^{-1})	10,000; 5,000

Table 3 Material properties of AZ61 alloy at different temperatures

Parameters	Values											
Temperature (°C)	20	200	300	400	500	566	600	632	680	700	730	800
Density (kg m^{-3})	1,780	1,756	1,742	1,728	1,714	–	1,637	–	–	1,561	–	1,547
Thermal conductivity (W m^{-1} $°C^{-1}$)	77	97	107	117	101	90	73	75	–	78	–	78
Viscosity (Pa s)	–	–	1,000	100	10	1	–	0.0012	0.0011	–	0.001	0.0009

(3) The contact between solidification shell and roller surface was assumed to be close. In the completely solid part of the contact surface, a small convective heat transfer coefficient (5,000 W $m^{-2}°C^{-1}$) [28] was assumed and a large convective heat transfer coefficient (10,000 W $m^{-2}°C^{-1}$) [28] was assumed for the other parts;
(4) The rollers had negligible deformation and rotated with constant speed;
(5) The plastic deformation heat resulting from rolling was assumed to be negligible compared to the heat in the magnesium alloy melt;
(6) The heat transfer mode in the roll-casting zone was considered to be a combination of conduction and convection. During the twin-roll casting, the convective heat transfer coefficient was assumed to remain unchanged. Radiative heat transfer was neglected.

The process parameters are listed in Table 2.

The main material properties considered were density, specific heat, viscosity, and thermal conductivity. These were determined by interpolation of the data in ref [29] and are listed in Table 3.

The "equivalent specific heat method" was used to account for the release of latent heat during the solidification process. The latent heat was added to the specific heat of magnesium alloy to yield an "equivalent specific heat," as shown in Eq. (1):

$$C_E = C_0 + \frac{L}{T_L - T_S} \tag{1}$$

C_E is the equivalent specific heat; C_0 is specific heat of magnesium alloy; L is latent heat of solidification; T_L *and* T_S are the liquidus and solidus temperatures, respectively. According to ref. [30], the latent heat of solidification of AZ61 magnesium alloy is 339,000 J kg^{-1} and the liquidus and solidus temperatures are 610 and 525 °C, respectively. Table 4 presents the amended equivalent specific heat of AZ61 magnesium alloy as a function of temperature.

3.2 Simulation models

The dimensions of the nozzle and roll-casting zone are shown in Fig. 4a. The vertical height of the nozzle is 30 mm, and the roller gap is 5 mm. A quarter of the overall physical domain was chosen for the computational domain, taking advantage of the two-axis symmetry. The computational mesh has to be such that it can accommodate the possibility of turbulence in the fluid flow field. An eight-node FLUID142 fluid element in ANSYS was adopted, and uniform hexahedral mesh generation was carried out. The FE meshing of the geometry is shown in Fig. 4b.

Conjugate heat transfer analysis enabled simultaneous determination of the temperature field in the solid regions and temperature and velocity fields in the fluid region. In the calculation, the momentum equation was solved using tri-diagonal matrix algorithm (TDMA) and the temperature-pressure equations were solved using pre-conditioned conjugate residual (PCCR) method. The relaxation factors of velocity, temperature, and pressure were set to 0.01; inertial relaxation factors were set to 1.0×10^{15}; simultaneously, the k–e turbulence model was activated during the transient solution.

A coupled calculation of fluid velocity and temperature fields in the magnesium alloy melt in the nozzle and the roll-casting zones was carried out, followed by calculation of temperature field in the rollers, and finally coupled calculation of the velocity and temperature fields in the rollers and magnesium alloy melt. Results of temperature fields calculated in the roll-casting zone were used as boundary conditions to impose the appropriate mechanical stress fields and thermal stress fields.

Table 4 Equivalent specific heat of AZ61 alloy at different temperatures

Temperature (°C)	300	400	500	565	566	600	632	635	700	800
Specific heat (J kg^{-1} $°C^{-1}$)	1,148	1,224	1,300	1,349	6,486	6,512	6,536	1,168	1,217	1,293

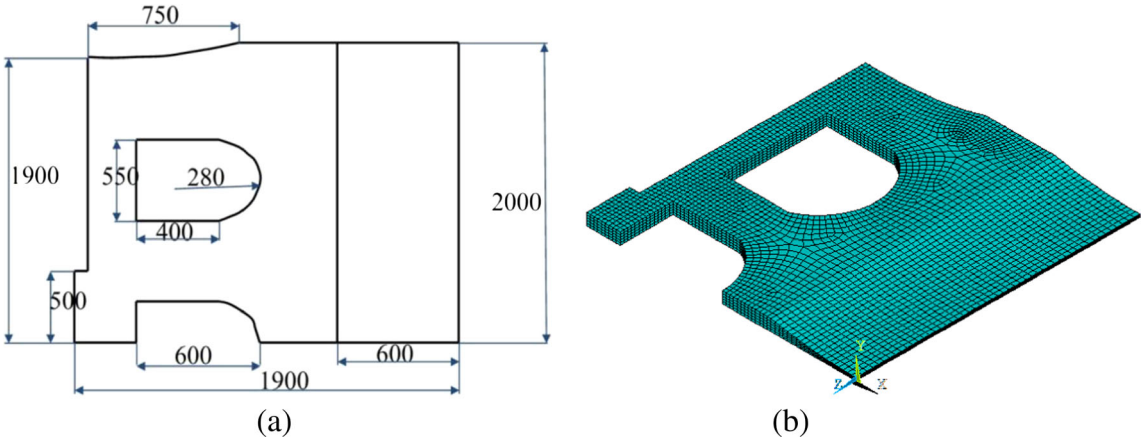

Fig. 4 **a** Model dimensions (mm) and **b** finite element mesh

4 Results and discussion

4.1 Experimental results

Twin-roll strip casting experiments were carried out with different pouring temperatures with a fixed casting velocity of 2.4 m/min. Figure 5a shows the AZ61 alloy strip produced by twin-roll casting at a pouring temperature of 680 °C. The casting could not be carried out continuously. Due to a low temperature in the nozzle and roll-casting zone, the flow of the magnesium alloy melt was affected. However, when the pouring temperature was increased to 710–720 °C, the operation could be carried out continuously. The cast strips are shown in Fig. 5b, c, respectively. An alloy strip of good surface quality could be obtained after dynamic adjustment of the process parameters. The main parameter that was adjusted was the casting velocity. Fine adjustment of the casting velocity kept the rolling pressure constant. Several experiments were carried out at a pouring temperature of 730 °C. Figure 5d shows the strips of AZ61 alloy at 730 °C. At this pouring temperature, the strip casting experiment could still be carried out, but the surface quality of strip was found to be very poor. Due to the high temperature, solidification of the emerging strip is delayed, resulting in strong surface oxidation.

Twin-roll strip casting experiments were carried out at different casting speeds with the pouring temperature fixed at 710 °C. Figure 6(*a1*) and (*a2*) shows the strips of AZ61 alloy corresponding to a casting speed of 1.8 m/min. This experiment could be carried out, but the strips were found to have some drawbacks, such as the hole in the middle of the strip shown in Fig. 6(*a1*). The magnesium alloy melt cools fast and the temperature distribution is not very uniform in the axial direction of the rollers in the roll-casting zone. Consequently, the relatively low temperature melt undergoes varying degrees of solidification, resulting in stoppage accompanied by formation of a hole. This hole is stretched in the rolling direction, and the blocking part is rolled out after a while. Another defect is large cracks at the edges, as shown in Fig. 6(*a2*). These cracks result from excessive cooling and uneven solidification. These two defects indicate that a casting speed of 1.8 m/min is too low. The experiment was therefore carried out at the higher casting speed of 2.4 m/min. Figure 6(*b1*) and (*b2*) shows the strips of AZ61 corresponding to a casting speed of 2.4 m/min. It was found that a strip with good surface quality could be produced successfully. Several

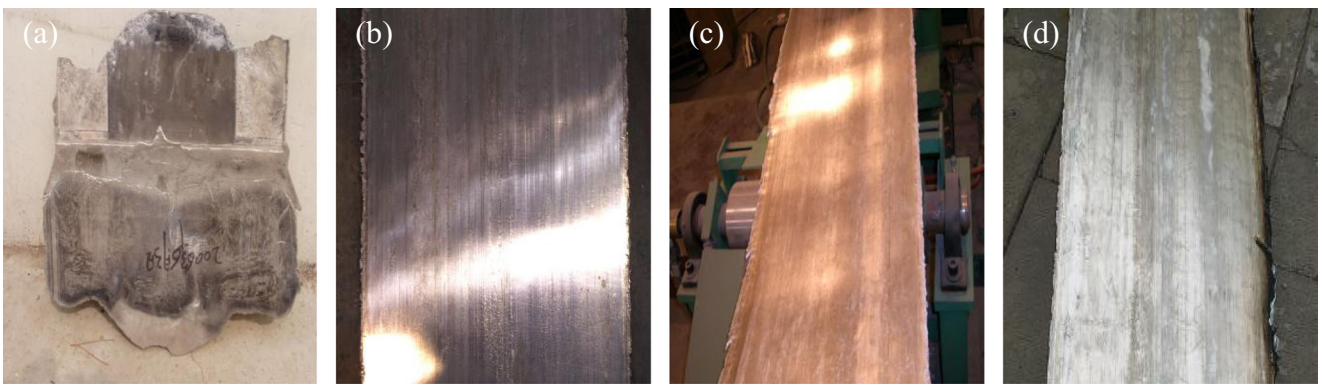

Fig. 5 Strips of AZ61 alloy by twin-roll casting at **a** 680, **b** 710, **c** 720, and **d** 730 °C

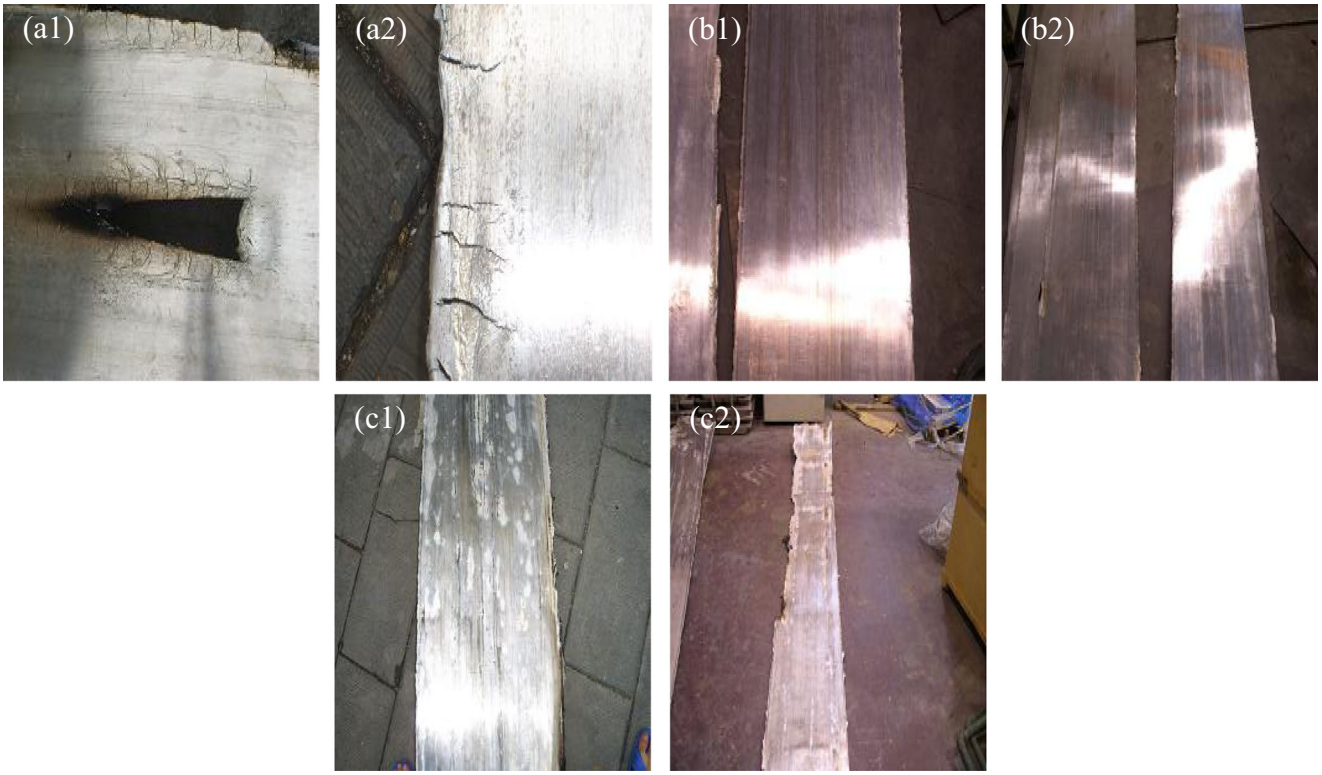

Fig. 6 Strips of AZ61 by twin-roll casting at **a** 1.8, **b** 2.4, and **c** 3.0 m/min

more experiments were carried out at a casting speed of 3.0 m/min. Figure 6(*c1*) and (*c2*) shows the strips of AZ61 corresponding to a casting speed of 3.0 m/min. These strips have poor surface features, such as darkened edges formed due to incomplete solidification and subsequent oxidation as the melt comes into contact with oxygen in the atmosphere. It was therefore concluded that a casting speed of 3.0 m/min was too high because at this casting speed, the magnesium alloy melt could not cool sufficiently.

4.2 Simulation results

Figure 7a–c shows the temperature fields in the magnesium alloy melt in nozzle, roll-casting zone, and near side dam when pouring temperature was specified to be 700 °C and the casting speeds were 1.8, 2.4, and 3.0 m/min, respectively.

Figure 7(*1*) shows the temperature fields in nozzle and roll-casting zone. Except for the edge region which is affected by the side dam, the temperature distribution in the cross section parallel to the rolling direction is uniform. With an increase in casting speed, the temperatures at strip surface and rolling exit zone show a remarkable rise, with the minimum temperature increasing from 334 to 416 °C. The temperature in the two-phase region of AZ61 alloy ranges from 525 to 610 °C. With an increase in casting speed, the two-phase region recedes from the biting end and moves towards the exit end. The length of two-phase region increases to some extent, with a corresponding reduction in the length of the solidification zone in contact with the roller surface. When the casting speed reaches 3.0 m/min, there are no solidification shells at the exit end of roll-casting zone except for fewer zones near the side dam. The result is that when the magnesium alloy melt leaves the roll-casting zone, it cannot form a strip. In the experiment, as shown in Fig. 6c, the actual pouring temperature was higher than that specified in the simulation, but an incomplete strip could still be produced. A possible reason is the high heat loss in practice while the melt alloy passes the nozzle. This heat loss was not considered in the simulation.

Figure 7(*2*) shows a cross-section view perpendicular to the roller axis of roller in the mid-plane of the model. The temperature distribution in the roll-casting zone is seen clearly. When the casting speed is 1.8 m/min, heat transfer between the magnesium alloy melt and roller surface is sufficient for the magnesium alloy melt to solidify completely while traveling towards the exit end. From this position to the exit end, the melt needs to withstand a large rolling force. The melt has high temperature, so its tensile strength is low. Under the action of the rolling force, the strip surface is prone to cracks. The lower the casting speed, the longer the completely solidified part, the farther the distance of solidification point to exit end, the higher rolling force withstood by the strip, the greater the tendency of crack formation. The process of roll casting is forced to be suspended due to stoppage resulting from complete and rapid solidification of magnesium alloy melt in the

roll-casting zone, as shown in Fig. 5a. On the other hand, when the casting speed is 2.4 m/min, the completely solidified region closely approaches the exit end. This situation does not retain a large rolling force and can ensure that the roll-casting process proceeds smoothly, resulting in a strip with better surface quality. When the casting speed reaches 3.0 m/min, heat transfer between the roller and the magnesium alloy melt is inadequate. The temperature of the melt at the exit end is higher than 525 °C, so that the melt in the two-phase region does not form a strip.

Figure 7(*3*) shows temperature fields in the roll-casting zone in the side dam. It can be seen that this area is cooler than the middle part due to heat transfer from three directions. With an increase in casting speed, the overall temperature of the side increases, the region undergoing complete solidification is shorter, and the two-phase region moves towards the exit end. It is seen that the melt undergoes complete solidification in the roll-casting zone, even when the casting speed reaches 3.0 m/min. It is obvious that over the region from the point of complete solidification to the exit end, the strip would have to withstand a large rolling force.

Figure 8a–c shows the temperature distributions in the magnesium alloy melt in the nozzle and roll-casting zones when the casting speed is 2.4 m/min and pouring temperatures are 680, 700 and 720 °C, respectively. With an increase in the pouring temperature, the temperatures at the strip surface and rolling exit end increase, with the minimum temperature rising from 370 to 389 °C. The two-phase region shifts towards the exit end and is stretched. The rise in pouring temperature has little effect on the cooling area affected by the side dam.

Figure 8(*2*) shows a cross-sectional view perpendicular to the roller axis in mid-plane of the model. With an increase in the pouring temperature, the depth of the casting cavity in the roll-casting zone increases slightly. The completely solidified region moves towards the exit end and is shorter. When the pouring temperature is 720 °C, the melt shows just a thin solidified shell while the material in the central region is two-phase. This results in a weaker strip that can fracture easily. This is shown in Fig. 5c in which the crack formation is more obvious compared to Fig. 5b.

Figure 9a–c shows the fluid (melt) flow fields in the nozzle and roll-casting zones when the pouring

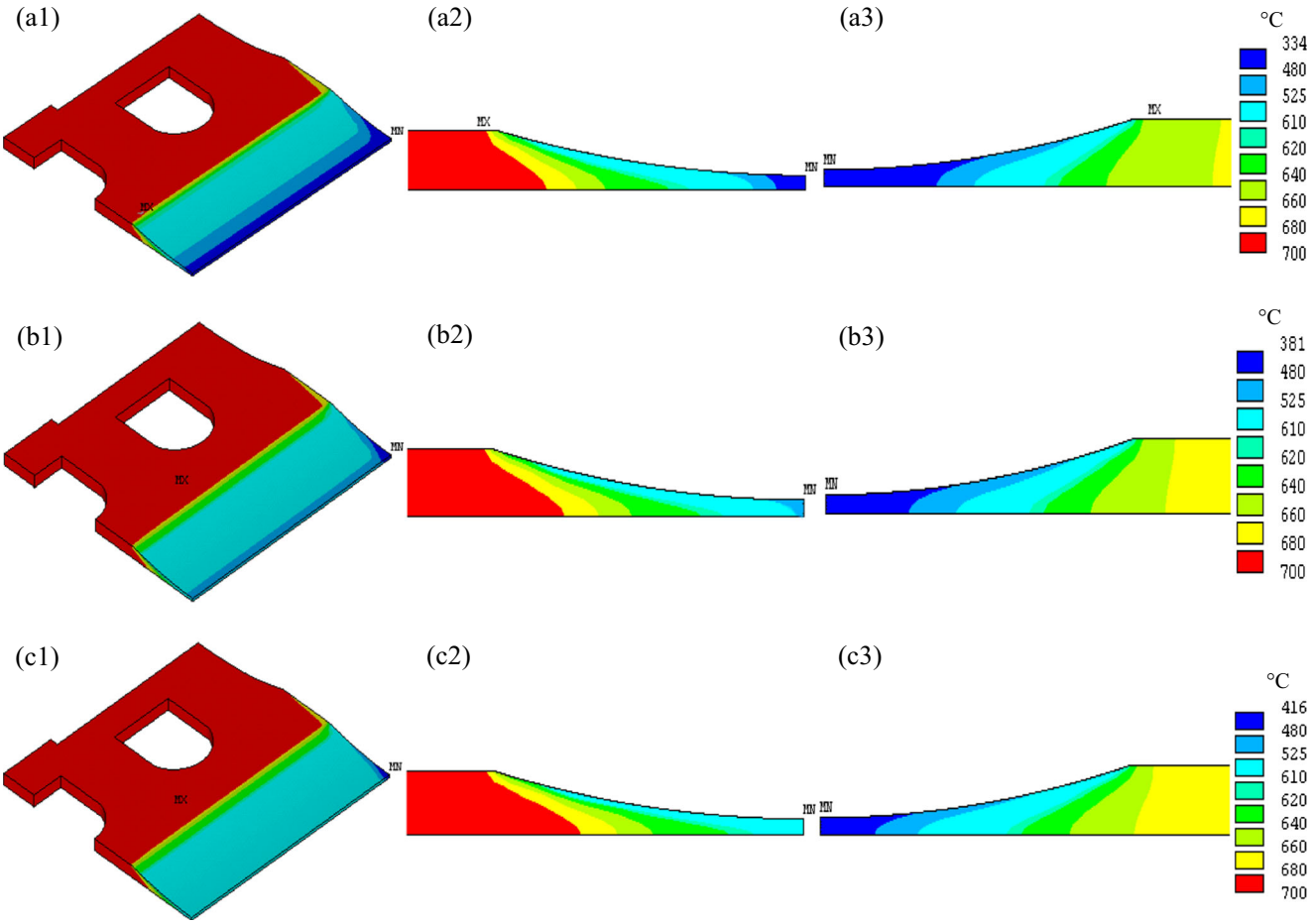

Fig. 7 Temperature fields of (*1*) nozzle and roll-casting zone, (*2*) roll-casting zone, and (*3*) near side dam at **a** v=1.8 m/min, **b** v=2.4 m/min, and **c** v=3.0 m/min

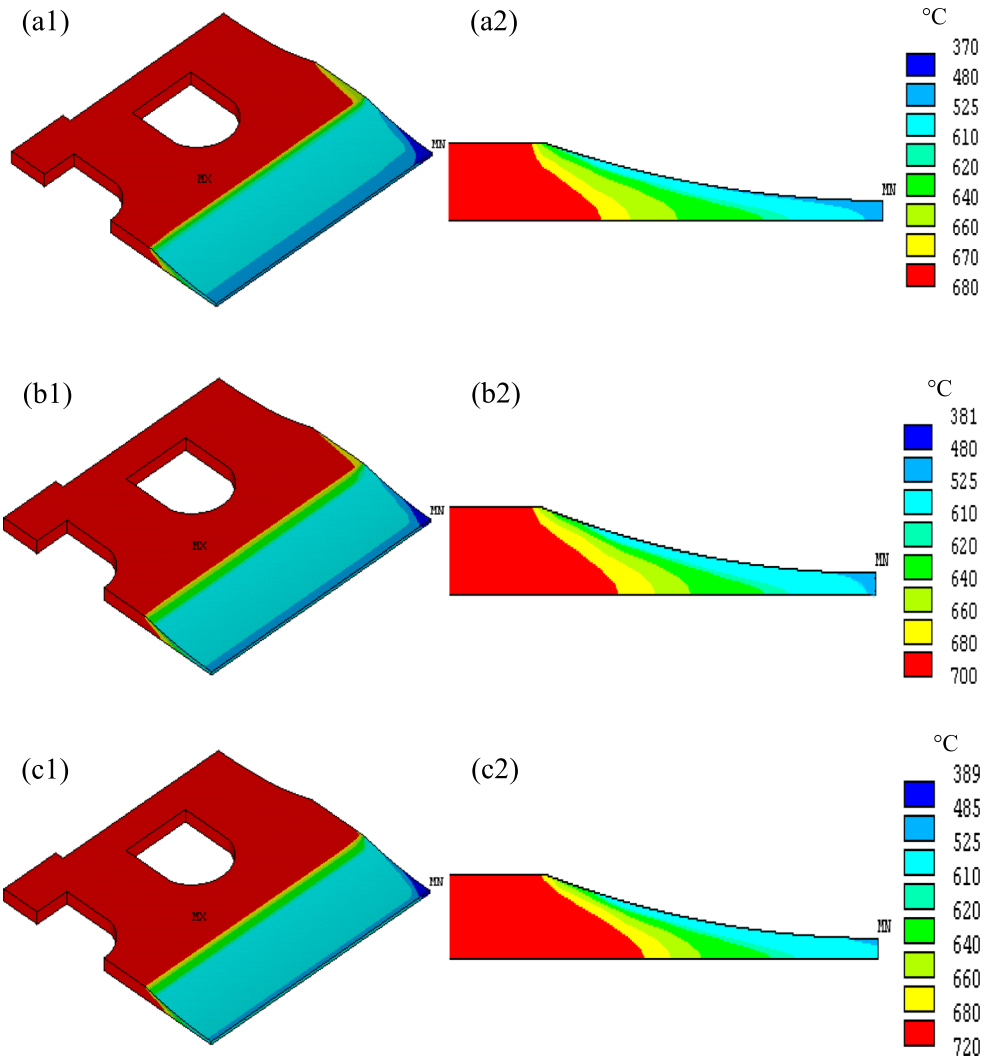

Fig. 8 Temperature fields of (*1*) nozzle and roll-casting zone and (*2*) roll-casting zone at **a** T= 680 °C, **b** T=700 °C, and **c** T= 720 °C

temperature is 700 °C and casting speeds are 1.8, 2.4, and 3.0 m/min, respectively. It can be seen that in the cases, the overall mobility trends of the melt are very similar. The melt flows into the nozzle at high velocity, through the spacer bypass, and uniformly into the roll-casting zone. The overall flow direction is towards the rolling exit end, and the lateral flow is weak. The melt flow region in front of the spacer is relatively small and is

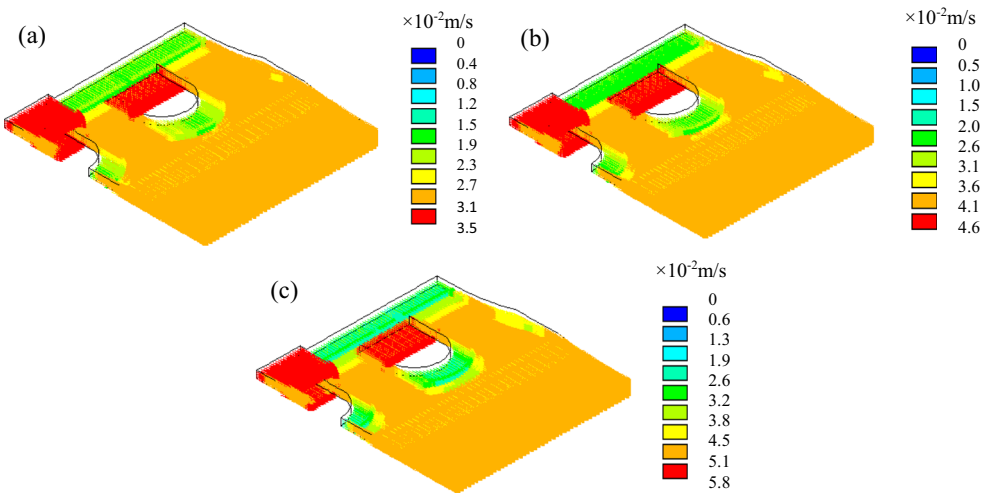

Fig. 9 Fluid flow fields in nozzle and roll-casting zone at **a** v= 1.8 m/min, **b** v=2.4 m/min, and **c** v=3.0 m/min

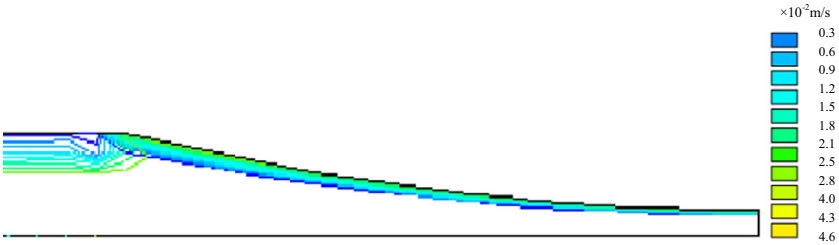

Fig. 10 Fluid (melt) flow field near the upper nozzle surface and roll-casting zone (casting speed 2.4 m/min)

elongated with an increase in casting speed. The overall flow becomes stronger with an increase in casting speed.

Figure 10 shows the fluid flow field in the vicinity of the upper surface of the nozzle and roll-casting zone when the casting speed is 2.4 m/min. It can be seen that a weak recirculating flow is formed when the melt flows out of the nozzle and into the roll-casting zone. A possible explanation is as follows: When the melt flows into the roll-casting zone, the temperature of the melt in contact with the roller surface decreases rapidly while moving at the speed of the roller surface (no-slip condition). With a reduction in the gap of the roll-casting zone, the melt flow velocity increases. The difference in flow speeds in different regions of the melt flow field leads to a recirculating flow near the entrance.

Figure 11a–c shows the fluid (melt) flow fields in the nozzle and roll-casting zones when the casting speed is 2.4 m/min and the pouring temperatures are 680, 700, and 720 °C, respectively. It can be seen that the flow fields are very similar. With an increase in pouring temperature, the overall flow speed increases while the slow-speed region in front of the spacer is elongated in the main flow direction.

Figure 12(*1*) shows the stress distributions in the roll-casting zone at a pouring temperature of 700 °C, with different casting speeds. In all cases, a uniform stress distribution is seen, except for the edges, with large stress concentration near the biting end. Compared with the temperature fields in Fig. 7(*1*), this region is where the melt changes from the liquidus phase to two-phase. Due to the release of latent heat, this region has large a thermal stress. With the increase of casting velocity, this region shrinks while the overall stress increases. When the casting velocity is 1.8 m/min, a stress concentration region with stress higher than 5 MPa is formed near the side dam, due to heat transfer. This is accompanied by a large temperature change. At a higher casting speed, the region affected by the heat transfer shrinks. When the casting velocity reaches 3.0 m/min, the region disappears completely. Figure 12(*2*) shows a cross-sectional view perpendicular to the roller axis in the model mid-plane. The stress distributions are very similar irrespective of the casting speed. Stress concentration occurs at the strip surface in contact with the roller surface, accompanied by a large temperature change in this area due to the cooling effect of the roller. Near the rolling exit end, the stress fields show significant differences. When the casting speed is 1.8 m/min, the stress concentration region is farthest from the exit end. Comparison in Fig. 7(*2*) shows that this area is in the vicinity of a region of complete solidification. The reason is a large temperature drop. With an increase in casting speed, the region of complete solidification moves towards exit end. When the casting speed is 2.4 m/min, this region along with the region of stress concentration reaches

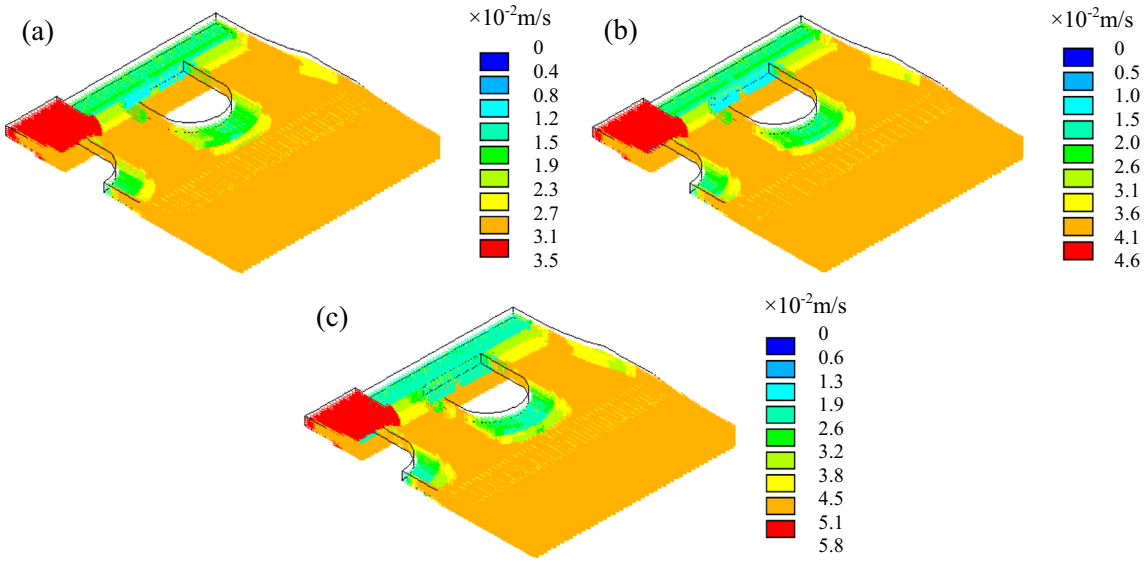

Fig. 11 Fluid (melt) fields in nozzle and roll-casting zone at **a** T=680 °C, **b** T=700 °C, and **c** T=720 °C

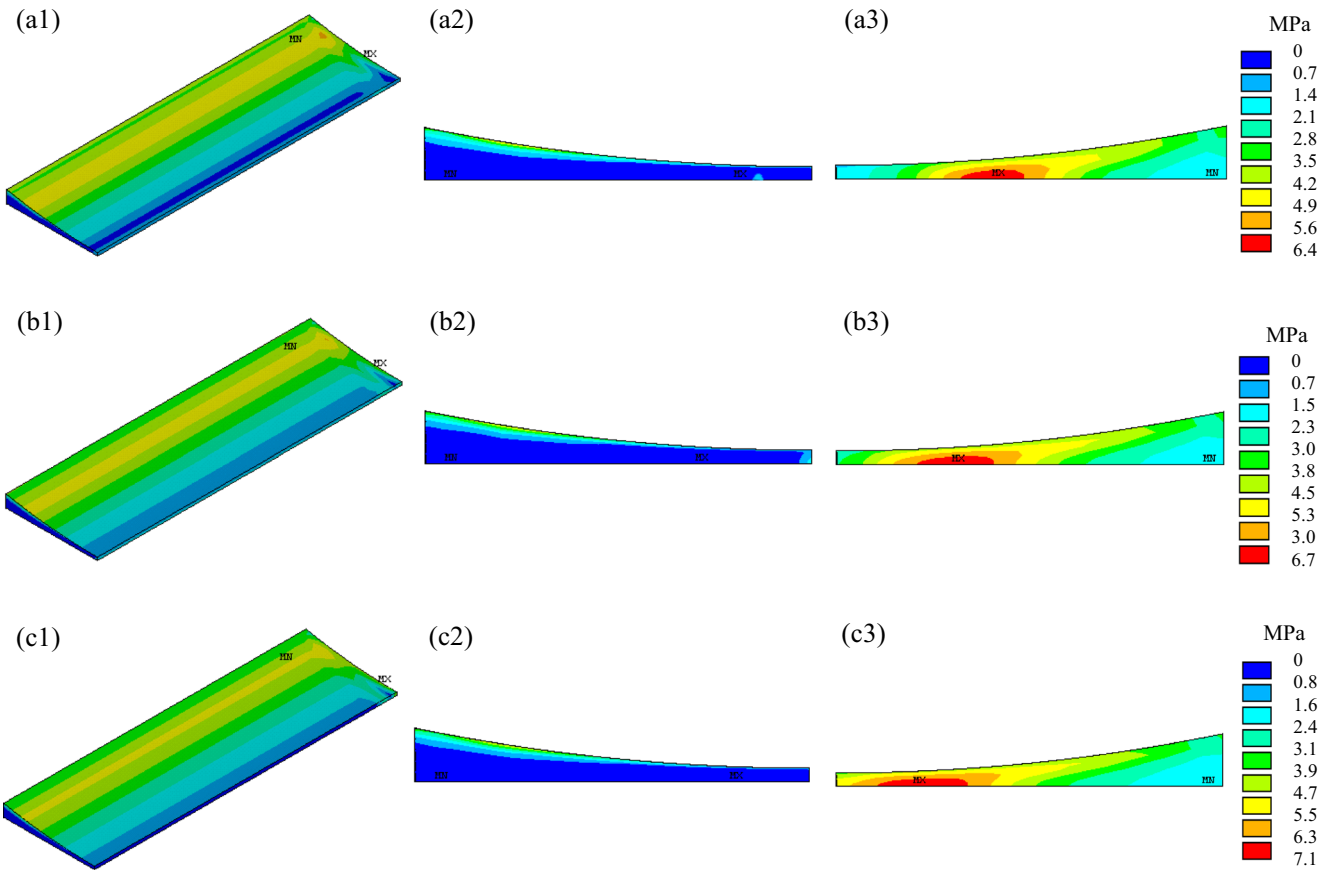

Fig. 12 Stress fields of roll-casting zone at **a** 1.8, **b** 2.4, and **c** 3.0 m/min

the exit end. When the casting speed is 3.0 m/min, both the completely solidified part and the stress concentration region disappear.

Figure 12(*3*) shows stress fields inside the side dam. This area undergoes cooling effect from three directions (side dam and two rollers) so that the temperature changes drastically. The maximum stress value in the overall roll-casting zone occurs here, with the stress level reaching 6~7 MPa. Comparison with the temperature fields in Fig. 7(*3*) shows that this area is in the vicinity of complete solidification region, and the temperature is about 500 °C. At this temperature, the tensile strength of AZ61 magnesium alloy is lower than 10 MPa [31]. This is a possible reason why cracks form relatively easily at the edge. In Fig. 6a, the edge has serious cracks. At higher casting speed, the complete solidification region moves towards the rolling exit end along with the stress concentration area. So an appropriate increase in casting velocity could prevent the area with large heat stress from having to withstand large rolling force, resulting in the formation and/or propagation of edge cracks.

Figure 13(*1*) shows stress distributions in the roll-casting zone at a casting speed of 2.4 m/min and different pouring temperatures. The large stress field still occurs at the start of the two-phase region. With an increase in pouring temperature, the area under large stress increases slightly. Higher stress concentration is seen near the side dam, with stress levels higher than 5 MPa. This happens for reasons mentioned above. It was seen in Fig. 8(*1*) that the effect of increasing the pouring temperature on the cooling area of the side dam is small. Therefore, when the pouring temperature rises, the extent of this stress concentration is still unchanged; it just moves a little towards the rolling exit end. Figure 13(*2*) shows a cross-section view perpendicular to the roller axis in the mid-plane of the model. In the three kinds of pouring temperatures, stress distributions in the roll-casting zone are similar. Due to the cooling effect of roller, strip surface contacting roller surface has violent temperature change and large stress. In the vicinity of rolling exit end, there is an area with a large stress level and the reason mentioned previously. With an increase in pouring temperature, this area moves a little towards the rolling exit end. It can be clearly seen that the effect of change of pouring temperature on stress distributions in roll-casting zone is not obvious.

Figure 13(*3*) shows stress distributions inside side dam. Due to this area affected by cooling of three directions, temperature changes dramatically and maximum stress value occurs, approximately 6~7 MPa. As in Fig. 5a, due to the

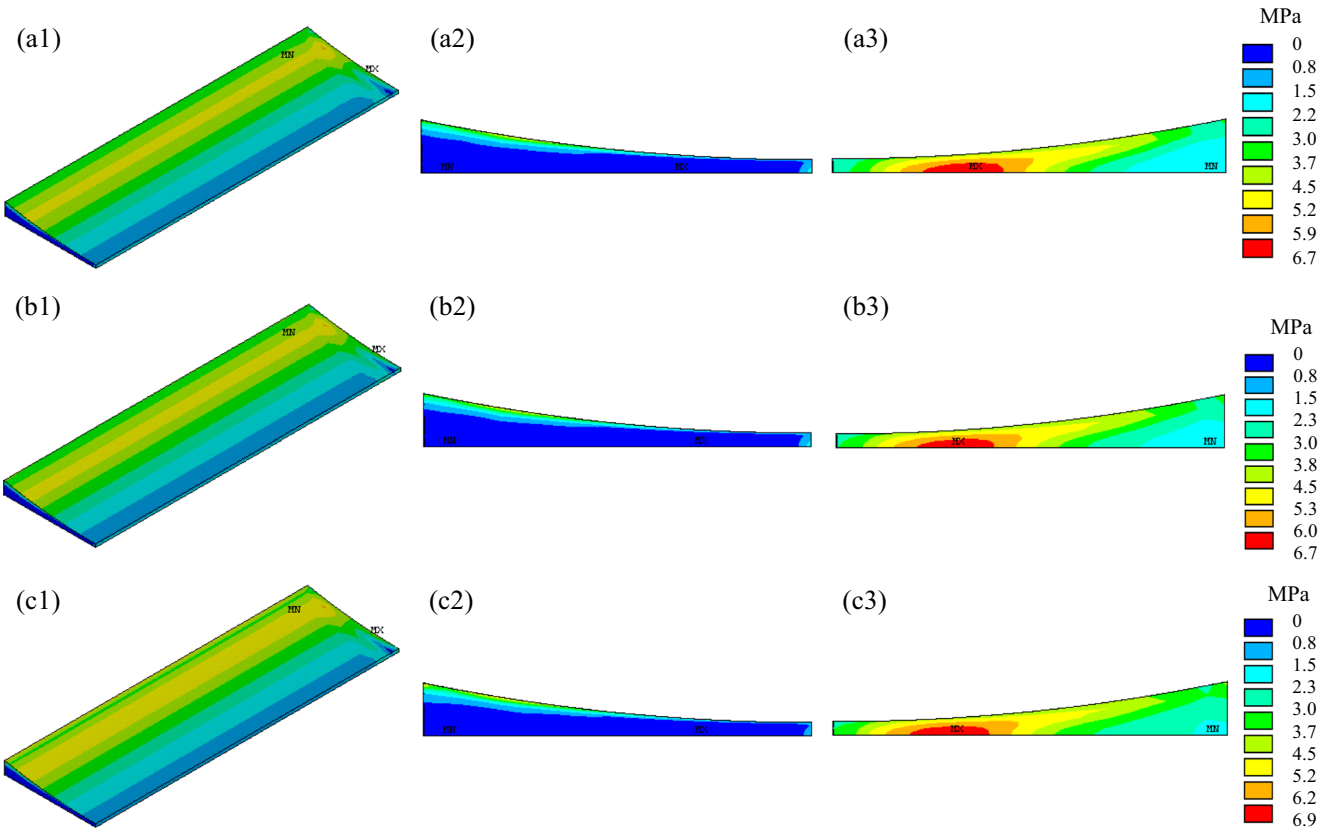

Fig. 13 Stress fields in the roll-casting zone at different pouring temperatures: **a** 680, **b** 700, and **c** 720 °C

heat loss being more in experiment, the maximum stress value exceeds the rolling pre-pressure and this result in stoppage. This area locates near complete solidification region. With an increase in pouring temperature, complete solidification region moves towards the rolling exit end and this area with maximum stress level also moves towards rolling exit end. So, an appropriate increase in pouring temperature can also prevent edge with large heat stress from having to withstand large rolling force and producing or enlarging edge cracks.

Figure 14 shows the exit temperatures of the melt close to the side dam at different casting velocities and pouring temperatures. A combination of experimental and simulation results can be used to determine the optimum exit temperatures and deduce the optimum pouring temperature and

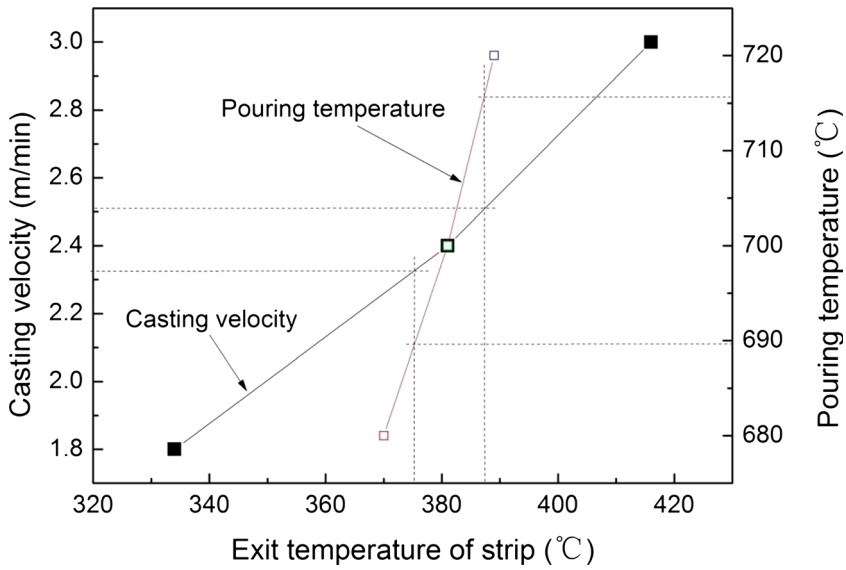

Fig. 14 Exit temperature at different casting velocities and pouring temperatures

casting velocity. The strip obtained at a pouring temperature of 720 °C and casting velocity 2.4 m/min, Fig. 5c, shows more cracks. The corresponding exit temperature is 389 °C, as shown in Fig. 8c. So, the upper limit of the exit temperature can be deduced as 388 °C. It is difficult to obtain a satisfactory strip with 680 °C and 2.4 m/min, as seen in Fig. 5a. The corresponding exit temperature is 370 °C, as shown in Fig. 8a. But, the strip obtained at 710 °C and 2.4 m/min, Fig. 5b, shows good surface quality. The corresponding exit temperature estimated from Fig. 14 is 385 °C. Consequently, the lower limit of the exit temperature can be deduced as ~375 °C. The optimum exit temperature is thus in the range from 375 to 388 °C. The corresponding optimum pouring temperature and casting velocity is in the range from 690 to 715 °C and from 2.3 to 2.5 m/min, respectively.

5 Conclusions

This paper presents a description of a series of experiments on twin-roll strip casting of an AZ61 magnesium alloy along with results of the corresponding numerical simulations of the process. The main objective was to optimize the process parameters, with particular focus on the pouring temperature and casting speed. The following general conclusions could be drawn:

(1) With an increase in casting speed from 1.8 to 3.0 m/min, the melt temperature at the rolling exit zone increases noticeably. The two-phase region recedes from the biting end and moves towards the rolling exit end. The distance between the completely solidified region and the rolling centerline is shortened, and the area affected by cooling of the side dam is smaller. If the casting speed is too low, the melt would have to withstand a larger rolling force and the possibility of crack formation increases. If the casting speed is too high, the melt would not be solidified completely at the rolling exit zone. The effect of pouring temperature on the temperature field in the nozzle and roll-casting zone is similar to that of the casting speed.

(2) The melt edge tends to solidify more easily than the center, which results in larger rolling force, stress concentration near the edge, and crack formation. An appropriate increase in casting velocity and pouring temperature would shift the stress concentration region closer to the rolling exit end and prevent occurrence and propagation of edge cracks.

(3) The results of the experiment and simulation indicate that for twin-roll strip casting of AZ61 magnesium alloy, the optimum pouring temperature is in the range from 690 to 715 °C and the casting speed in the range from to 2.5 m/min.

Acknowledgments One of the authors (HLY) gratefully acknowledges financial support from the Vice-Chancellor's Fellowship Grant at the University of Wollongong, Australia, and from the National Natural Science Foundation of China through Grant 51105071.

References

1. Li DN, Luo JR, Wu SS, Xiao ZH, Mao YW, Song XJ, Wu GZ (2002) Study on the semi-solid rheocasting of magnesium alloy by mechanical stirring. J Mater Process Technol 129: 431–434
2. Yoshihara S, Yamamoto H, Manabe K, Nishimura H (2003) Formability enhancement in magnesium alloy deep drawing by local heating and cooling technique. J Mater Process Technol 143–144: 612–615
3. Haga T, Kapranos P (2002) Billetless simple thixoforming process. J Mater Process Technol 130–131:581–586
4. Haga T, Kapranos P (2002) Simple rheocasting processes. J Mater Process Technol 130–131:594–598
5. Haga T, Nishiyama T, Suzuki S (2003) Strip casting of A5182 alloy using a melt drag twin-roll caster. J Mater Process Technol 133:103–107
6. Haga T, Suzuki S (2003) Melt ejection twin roll caster for the strip casting of aluminium alloy. J Mater Process Technol 137:92–95
7. Watari H, Koga N, Davey K, Haga T, Alonso Ragado MT (2006) Warm deep drawing of wrought magnesium alloy sheets produced by semi-solid roll strip-casting process. Int J Mach Tool Manu 46:1233–1237
8. Watari H, Koga N, Paisarn R, Haga T (2004) Formability of magnesium alloy sheets manufactured by semi-solid roll strip casting. Mater Sci Forum 449–452:181–184
9. Watari H, Haga T, Koga N, Davey K (2007) Feasibility study of twin roll casting process for magnesium alloys. J Mater Process Technol 192–193:300–305
10. Jiang B, Liu WJ, Qiu D, Zhang MX, Pan FS (2012) Grain refinement of Ca addition in a twin-roll-cast Mg-3Al-1Zn alloy. Mater Chem Phys 133:611–616
11. Masoumi M, Zarandi F, Pekguleryuz M (2011) Microstructure and texture studies on twin-roll cast AZ31 (Mg-3 wt.% Al-1 wt.% Zn) alloy and the effect of thermomechanical processing. Mater Sci Eng A 528:1268–1279
12. Zhao H, Li PJ, He LJ (2012) Microstructure and mechanical properties of an asymmetric twin-roll cast AZ31 magnesium alloy strip. J Mater Process Technol 212:1670–1675
13. Zhao H, He LJ, Li PJ (2011) Microstructure of asymmetric twin-roll cast AZ31 magnesium alloy. Trans Nonferrous Met Soc China 21: 2372–2377
14. Bayandorian I, Huang Y, Fan Z, Pawar S, Zhou X, Thompson GE (2012) The impact of melt-conditioned twin-roll casting on the downstream processing of an AZ31 magnesium alloy. Metall Mater Trans A 43A:1035–1047
15. Mino T, Asakawa M, Lee D, Fujiwara T, Matsuzaki K, Kobayashi M (2006) Twin-roll strip casting of AZ61 magnesium alloy and improvement of formability by structure-control rolling. J Mater Process Technol 177:534–538
16. Liang D, Cowley CB (2004) The twin-roll strip casting of magnesium. JOM 56:26–28
17. Hwang JD, Lin HJ, Jang JSC, Hwang WS, Hu CT (1996) Relationship between flow characteristics and surface quality in inclined twin roll strip casting. ISIJ Int 36:690–699
18. Santos CA, Spim JA Jr, Garcia A (2000) Modeling of solidification in twin-roll strip casting. J Mater Process Technol 102:33–39

19. Lin HJ (2004) Modelling of flow and heat transfer in metal feeding system used in twin roll casting. Modelling Simul Mater Sci Eng 12: 255–272
20. Ju DY, Zhao HY, Hu XD, Ohori K, Tougo M (2005) Thermal flow simulation on twin roll casting process for thin strip production of magnesium alloy. Mater Sci Forum 488–489:439–444
21. Miao YC, Zhang XM, Di HS, Wang GD (2006) Numerical simulation of the fluid flow, heat transfer, and solidification of twin-roll strip casting. J Mater Process Technol 174:7–13
22. Bae JW, Kang CG, Kang SB (2007) Mathematical model for the twin roll type strip continuous casting of magnesium alloy considering thermal flow phenomena. J Mater Process Technol 191:251–255
23. Zeng J, Koitzsch R, Pferfer H, Friedrich B (2009) Numerical simulation of the twin-roll casting process of magnesium alloy strip. J Mater Process Technol 209:2321–2328
24. Zhao H, Li PJ, He LJ (2011) Coupled analysis of temperature and flow during twin-roll casting of magnesium alloy strip. J Mater Process Technol 211:1197–1202
25. Xu GM, Wang DG, Li JT, Cui JZ (2009) Effects of rolling process on microstructure and properties of twin rolling-casting AZ61 magnesium alloy strip. Special Cast Nonfer Alloy 29(7):599–600
26. Li JT, Xu GM, Wang YB, Cui JZ (2009) Effect of twin roll-casting on microstructure and performance of hot rolling Mg-5.45 % Al-1.36 % Si magnesium alloy plate. Mater Mech Eng 33(10):72–74
27. Li JT, Xu GM, Yu HL, Su LH, Deng GY, Lu C, He LZ, Li HJ (2012) Optimization and application of process parameters in an AZ61 alloy twin-roll strip casting. 15th International Conference on Advances in Materials & Processing Technologies, Wollongong
28. Wu D (2008) Study on technics of twin-roll casting of AZ61 magnesium alloy. Northeastern University, Shenyang
29. Michael MA, Hugh B (1999) Magnesium and magnesium alloys. ASM International, Materials Park, pp 258–260
30. Портни КИ, Лебедев АА, Lin P (1959) Handbook of magnesium alloys. Metallurgical Industry Press, Beijing, pp 303–308, translated
31. Li WX (2005) Magnesium and magnesium alloys. Central South University Press, Hunan, pp 138–140